# Brain Tumor Segmentation and Classification from MRI Images using Improved FLICM Segmentation and SCA Weight Optimized Wavelet-ELM Model

Debendra Kumar Sahoo[1]
Ph.D Scholar, Dept. of ECE
Centurion University of Technology and Management, Bhubaneswar
Odisha, India

Satyasis Mishra[2]*
Dept. of ECE
Centurion University of Technology and Management, Bhubaneswar
Odisha, India

Mihir Narayan Mohanty[3]
Dept. of ECE
SOA University
Odisha, India

***Abstract*—Image segmentation is an essential technique of brain tumor MRI image processing for automated diagnosis of an image by partitioning it into distinct regions referred to as a set of pixels. The classification of the tumor affected and non-tumor becomes an arduous task for radiologists. This paper presents a novel image enhancement based on the SCA (Sine Cosine Algorithm) optimization technique for the improvement of image quality. The improved FLICM (Fuzzy Local Information C Means) segmentation technique is proposed to detect the affected regions of brain tumor from the MRI brain tumor images and reduction of noise from the MRI images by introducing a fuzzy factor to the objective function. The SCA weight-optimized Wavelet-Extreme Learning Machine (SCA-WELM) model is also proposed for the classification of benign tumors and malignant tumors from MRI brain images. In the first instance, the enhanced images are undergone improved FLICM Segmentation. In the second phase, the segmented images are utilized for feature extraction. The GLCM feature extraction technique is considered for feature extraction. The extracted features are aligned as input to the SCA-WELM model for the classification of benign and malignant tumors. The following dataset (Dataset-255) is considered for evaluating the proposed classification approach. An accuracy of 99.12% is achieved by the improved FLICM segmentation technique. The classification performance of the SCA-WELM is measured by sensitivity, specificity, accuracy, and computational time and achieved 0.98, 0.99, 99.21%, and 97.2576 seconds respectively. The comparison results of SVM (Support Vector Machine), ELM, SCA-ELM, and proposed SCA-WELM models are presented to show the robustness of the proposed SCA-WELM classification model.**

***Keywords*—Sine cosine algorithm; extreme learning machine; fuzzy c means; GLCM feature; support vector machine**

## I. Introduction

Brain tumor-related deaths are increasing worldwide according to the reports of the WHO (World Health Organization). The people affected by brain tumors are suffered from the symptoms of headache, vomiting, mildness of eye vision, and many more as per the medical study. The early treatment of tumor-related disease is essential to avoid recurrent deaths. To make treatment faster, automated segmentation and classification techniques are the requirements for medical diagnosis. The pre-processing step is simple and essential in brain-image analysis. Pre-processing is generally used to reduce the noise and enhance the image resolution and contrast. Many pre-processing approaches are used, like un-sharp masking, veneer filters as well as median-filters. Median filters are usually utilized during the pre-processing phase to protect the boundaries of an image [1]. The image segmentation of brain tumors from "magnetic resonance imaging (MRI)" is a significant assignment for the medical diagnosis of brain tumors. The conventional fuzzy c-means clustering (FCM) algorithm is sensitive to noise. This paper proposes an improved fuzzy local information-based FCM image segmentation to address the difficulties of segmentation. Sehgal et al. [2] proposed a segmentation strategy based on neural network optimization that uses neighborhood attraction using MRI. By taking into account the local attractiveness, the strategy changed the classic FCM method. The enhanced FCM clustering (IFCM), takes into account local attractions, based on two components: characteristics as well as a span of attraction. To partition brain tumor MRIs, researchers used the method published by Nabizadeh et al. [3] for calculating characteristics from the association between the tumors and with brain's LaVs. The method is divided into 4 steps: pre-processing, segmentation, and feature extraction with classification. Li et al. [4] suggested a brain tumor partition technique that incorporated anisotropic diffusion filtering as a pretreatment step, followed by partition as well as tumor extraction utilizing region with circularity using the FCM technique.

Machine learning has ignited considerable interest in modern computers in the field of medicine. In the area of brain-tumor recognition, a variety of advanced machine learning approaches are applied. Advanced methods are employed to identify the use of brain pictures and improve the quality of the information collected, such as image labeling, image reconstruction, skull removal, and registration [13]. As a result, machine learning has enabled clinics, engineers, and computer scientists to collaborate to develop semi-automated and eventually completely automated tumor diagnostic systems with improved accuracy and processing speed. Motivated by

*Corresponding Author.

the advancements of machine learning, we have proposed the following contributions.

### A. Contribution of the Research Work

Three contributions are proposed based on image enhancement, image segmentation, and classification. The contributions are summarized as follows:

- In the first aspect, the position and velocity parameters of the SCA algorithm are modified to enhance the quality of the images.
- In the second aspect, the fuzzy factor in FLICM segmentation is replaced with a new fuzzy factor to improve the tumor detection and noise reduction capability from the brain MRI images. The mathematical analysis for the improved fast and robust FLICM segmentation algorithm is presented to authenticate the proposed segmentation.
- In the third aspect, the weights of the Mexican Hat Wavelet -ELM model optimization by the SCA optimization technique are proposed to enhance the classification performance.

The paper is organized as follows. Section 2 presents the research implementation diagram, Section 3 presents the Sine cosine algorithm for image enhancement, the proposed fast and robust FLICM segmentation technique and proposed SCA-WELM model explanation, and Section 4 presents results and discussion of the proposed image enhancement, segmentation, and classification, Section 5 presents the conclusion and followed by the references.

## II. Related Work

Several segmentation techniques are presented by the researchers, and some of the latest research is included in the related work. Pinheiro et al. [5] devised a novel MRI technique for detecting brain tumors. Global threshold partitioning has been applied after pre-processing of input MRIs. Before watershed partition, Morphological approaches have been used to improve its results. Elazab et al. [6] proposed an "adaptively regularized kernel-based fuzzy C-means (ARKFCM)" segmentation to reduce computational time than the KFCM segmentation. FCM clustering algorithms with spatial constraints are proposed to remove the noise proposed in [7,8]. Chao et al. [9] proposed a GM-ARKFCM algorithm to show better segmentation than ARKFCM. Cherfa et al. [10] proposed AKFRFCM using Particle swarm optimization to improve segmentation capability. Tao Lei et al [11] presented a "fast and robust FCM (FRFCM)", which uses more parameters, and fails drastically to reduce Gaussian noise, beyond 30%. Satyasis et al. [12] proposed an improved fast and robust FCM algorithm (IFRFCM) to improve the noise reduction capability. Belean et al. [14] proposed a density-based spatial clustering procedure driven by a level-set approach for microarray spot segmentation and quality measures were obtained. Wenxiu et al. [15] proposed a two-phase selective segmentation method, in which the first phase reduces noise on segmentation and the second phase shows the selective segmentation on the preprocessed image.

There are several machine learning methodologies and methods to detect brain tumors by utilizing MRIs. An approach has been described by El-Dahshan et al. [16], during the discovery phase, an artificial feedback neural network and KNN are used. Saritha et al. [17] explained a new method for identifying usual and unusual brain MRI images pathologically. Three features are extracted using wavelet entropy-based spider-web plots. Yang et al. [18] suggested a recent method for MRI-based early recognition of brain tumors. With the RBF function, a kernel-type SVM is used as a classifier. In [19], Kalbkhani et al. employed 2D DWT and generalized autoregressive conditional heteroskedasticity (GARCH). The features are extracted using linear discriminate analysis (LDA), and the feature vectors are reduced using PCA. For the detection process, KNN, as well as SVM identifiers, are used. A method for tumor detection was proposed by Xiao [20] and Abd-Ellah et al. [21]. The input image is used to extract three kinds of characteristics: intensity-based, texture-based, and symmetry-based features. Mohsen et al. [22] employed a recent MRI method for recognizing brain tumors. For dimensionality reduction, PCA is utilized to reduce picture features. A BPNN determines if a subject's pictures are normal or irregular. Soltaninejad et al. [23] suggested a mixed method for MRI recognition of brain tumors. A feedback pulse-coupled neural network is used to preprocess the image (FPCNN). For feature extraction and reduction, PCA and the discrete wavelets transform (DWT) are employed. Using two-level DWT decomposition, the LL sub-band data is delivered to the PCA. For the detection stage, PCA has been utilized to choose a vector of seven features. The FFBPNN is then used to identify whether or not the MRI image is usual or unusual. Abdel-Maksoud et al. gave a new approach for detecting brain tumors using MRIs in [24]. A median filter is used to preprocess MRI images before DWT extracts features. PCA has been used to reduce the number of features, whereas RBF and kernel type SVM has been used to recognize them. Tustison et al. [25] extracted features using Daubechies wavelets, which were subsequently processed using PCA to decrease feature vectors.

The usual and unusual MRIs haave then detected utilizing an SVM as well as RBF. Nabizadeh et al. [26] described a hybrid method to recognize brain tumors utilizing MRIs. The suggested approach involves LS-SVM, GLCM, and noise filtering in three levels: preprocessing, and feature extraction with detection. The four features collected are energy, correlation, homogeneity, and contrast. Huang et al. [27] discovered that the brain MRI dataset is studied using MLP, LVQ, RBF, and SOM classifiers in the recognition step. Median, as well as Gaussian filters are utilized during preprocessing state. Boarder could be extracted by utilizing Gaussian thresholding. GLCM has been utilized to extract features, which results in 21 features that are then reduced to 8 by PCA. Mahima et al. [28] proposed a fractional order contour detection PDE (partial differential equation) model with a regularization term for noise reduction and maintaining the regularity of level set function (LSF). A cellular neural network (CNN) model is used to solve the proposed contour detection PDE. Bogdan et al. [29] proposed an edge-based active contour model (ACM) driven by cellular neural networks (CNNs) for the segmentation procedure. Javeria et al.

[30] proposed the inceptionv3model for deep feature extraction, and quantum variational classifier (QVR) with the 2020-BRATS dataset and achieved more than 90% detection accuracy. Muhammad et al. [31] proposed Berkeley's wavelet transformation (BWT) and deep learning classifier and achieved an accuracy of 98.5%. Ramin et al. [32] Proposed Cascade Convolutional Neural Network (C-ConvNet/C-CNN) classifier with the BRAT-2018 dataset and achieved a dice score of 0.9113 for enhancing tumor. Isselmou et al. [33] deep wavelet autoencoder model with 2500 MR brain images of brat dataset and achieved an accuracy of 99.3% and 0.1 loss validation.

## III. Methodology

### A. Research Flow Diagram

The research work follows the following steps: (i) The Dataset-255 brain tumor images are collected and the SCA technique is applied for image enhancement and segmented by the novel Improved FLICM segmentation techniques. Further (ii) the segmented images undergo GLCM feature extraction; (iii) in the third stage, the extracted features are fed as input to the proposed SCA weight optimized WELM model for the classification of the benign and malignant tumors; (iv) in the fourth stage classification comparison results of the models are presented. The research implementation phase is shown in Fig. 1.

### B. The Sine Cosine Algorithm (SCA)

Swagat et al. [34] proposed PSO and APSO algorithms for enhancement of the gray images, but not applied to brain tumor images. The "sine cosine algorithm" (SCA) [35] is an optimization algorithm based on the sine and cosine functions search also not utilized for brain MRI image enhancement.

According to sine cosine algorithm [35] the position equation is updated as

$$X_i^{n+1} = \begin{cases} X_i^n + \alpha_1 \times sin(\alpha_2) \times |\alpha_3 p^{gbest} - X_i^n|, \alpha_4 < 0.5 \\ X_i^n + \alpha_1 \times cos(\alpha_2) \times |\alpha_3 p^{gbest} - X_i^n|, \alpha_4 \geq 0.5 \end{cases} \quad (1)$$

Where $\alpha_1, \alpha_2, \alpha_3, \alpha_4$ are the random variables and $\alpha_1$ is given by.

$$\alpha_1 = a\left(1 - \frac{n}{K}\right) \quad (2)$$

Where " is the current iteration, K is the maximum number of iterations". $p^{gbest}$ is the global best position of the pixels in the image.

The $X_i^n$ signifies the "current position" and $X_i^{n+1}$ signifies the "new position". The $\alpha_1$ is the next position in the search, $\alpha_2$ determines direction of movement, $\alpha_3$ controls the current movement, and the parameter $\alpha_4$ uniformly switches among the sine and cosine functions. The parameter and $\alpha_1$ is given by.

$$\alpha_1 = a\left(1 - \frac{n}{K}\right)$$

Where the current iteration is given by $n$ , maximum numbers of iterations are denoted by K and $a$ is a constant. Now considering the population images Xi as corresponded image position $\xi_i$ in the image and applies the SCA algorithm for image enhancement.

$$\xi_i^{n+1} = \begin{cases} \xi_i^n + \alpha_1 \times sin(\alpha_2) \times |\alpha_3 p^{gbest} - \xi_i^n|, \alpha_4 < 0.5 \\ \xi_i^n + \alpha_1 \times cos(\alpha_2) \times |\alpha_3 p^{gbest} - \xi_i^n|, \alpha_4 \geq 0.5 \end{cases} \quad (3)$$

With the equation operation on the image, the new position of the pixel values of the images is calculated for image enhancement. The pseudo code for the algorithm implementation is presented in Table I.

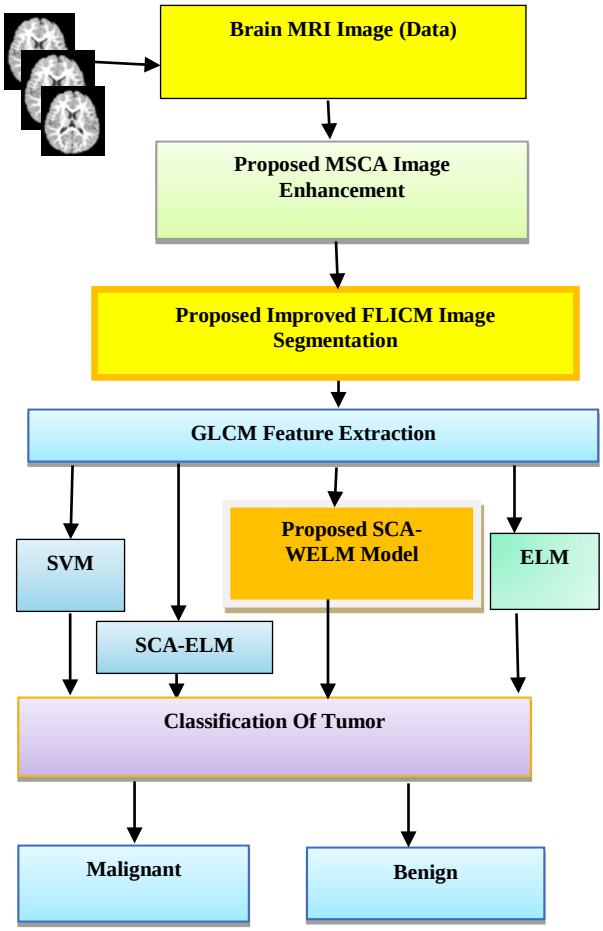


Fig. 1. Research Flow Diagram.

TABLE I. Pseudo Code: SCA Algorithm Implementation for Image Enhancement

| **Pseudo code: SCA Algorithm implementation for Image** |
|---|
| 1. Initialize random position and velocity vectors. |
| 2. Initialize the SCA parameters $\alpha_1, \alpha_2, \alpha_3, \alpha_4$ |
| 3.Evaluate the evaluate fitness based on $x_{ii}$ |
| 4.%optimization loop |
| 5.for i=1:k |
| 6. update SCA parameter to obtain fitness |

7. update the modified position and velocity equation

$$\xi_i^{n+1} = \begin{cases} \xi_i^n + \alpha_1 \times sin(\alpha_2) \times |\alpha_3 p^{gbest} - \xi_i^n|, \alpha_4 < 0.5 \\ \xi_i^n + \alpha_1 \times cos(\alpha_2) \times |\alpha_3 p^{gbest} - \xi_i^n|, \alpha_4 \geq 0.5 \end{cases} \quad (4)$$

8. end for the loop i
9.Stopping criteria: getting fitness as optimal solution

### C. Improved Fast and Robust Fuzzy Local Information C Means (FRFLICM) Algorithm

According to enhanced fuzzy c means EnFCM [36] algorithm the image $\xi$ is considered from the original image and is given by.

$$\xi_k = \frac{1}{\alpha}\left(x_k + \frac{\alpha}{N_k}\sum_{j \in N_k} x_j\right) \quad (5)$$

Where the gray value of $k^{th}$pixel of image $\xi$ is given by $\xi_k$, $x_j$ is neighbors of $x_k$, $N_k$ is set of neighbors around $x_k$. Now the new objective function is given by.

$$J_s = \sum_{l=1}^{N}\sum_{k=1}^{c} \gamma_l \, u_{kv}^m \|\xi_l - v_k\|^2 \quad (6)$$

Where " $u_{il}$ represents the fuzzy membership of gray value $l$." $\gamma_l$ is the number of the pixels having the gray value equal to$l$, and $l = 1,2,\ldots.N$.

According to the FLICM segmentation [37], the fuzzy factor is given by.

$$G_{kv} = \sum_{\substack{k \in N_v \\ v \neq k}} \frac{1}{d_{vk}+1}(1 - u_{kv})^m \|x_v - v_k\|^2 \quad (7)$$

To improve the noise reduction capability the fuzzy factor is modified, and the new cost function is given by with improved fuzzy factor as.

$$J_s = \sum_{l=1}^{N}\sum_{k=1}^{c} \gamma_l \, u_{kv}^m \|\xi_l - v_k\|^2 + \sum_{v=1}^{N}\sum_{k=1}^{c} {G_{kv}}^2 \quad (8)$$

$$J_s = \sum_{l=1}^{N}\sum_{k=1}^{c} \gamma_l \, u_{kv}^m \|\xi_l - v_k\|^2 + \sum_{v=1}^{N}\sum_{k=1}^{c} \left(\sum_{\substack{k \in N_v \\ v \neq k}} \frac{1}{d_{vk}+1}(1 - u_{kv})^m \|x_v - v_k\|^2\right)^2 \quad (9)$$

With the new objective function, the segmentation accuracy has been improved and segmentation results are presented in the result section.

### D. Wavelet ELM Model with SCA Optimization

In this research work, we propose an SCA optimization for wavelet ELM weight optimization (SCA-WELM) that learns the output weights of the ELM classifier. The pseudo-code for SCA weight optimization of the WELM model is presented in Table II. The SCA-WELM model with hidden and output layers is shown in Fig. 2.

The output function of ELM [38] with $L$ hidden neurons is represented by.

$$y = \sum_{k=0}^{L} \beta_k h_k(w_k; x) \quad (10)$$

where $h(w; x) = [1, h_1(w_1; x), \ldots\ldots, h_L(w_L; x)]$ is the hidden feature mapping and $\beta$ is the weight vector of all hidden neurons to an output neuron, $h_k(\cdot)$is the activation function of hidden layer. Equation (10) can be written as.

$$H\beta = y \quad (11)$$

Where $H$ is the $N \times (L+1)$hidden layer feature-mapping matrix, whose elements are as follows:

$$H = \begin{bmatrix} 1 & h_1(w_1; x_1) & \cdots & h_L(w_N; x_1) \\ \vdots & \vdots & \vdots & \vdots \\ 1 & h_1(w_1; x_N) & \cdots & h_L(w_N; x_N) \end{bmatrix} \quad (12)$$

And $h_L(w_N; x_N) = [w_1 x_1 + w_1 x_1 \ldots\ldots\ldots w_N x_N].\varphi(t)$

Where $\varphi(t) = c(1 - x^2)exp\left(-\frac{x^2}{2}\right)$ and $c = \left(\frac{2}{\sqrt{3}}\pi^{-1/4}\right)$

Equation (10) is a linear system, which is solved by

$$\beta = H^{\dagger} d, \qquad H^{\dagger} = (H^T H)^{-1} H^T \quad (13)$$

Where $H^{\dagger}$ is the "Moore–Penrose generalized inverse of matrix $H$ " and $d = [d_1, \ldots\ldots, d_N]^T$.

And $d = \begin{bmatrix} d_1 \\ d_2 \\ \vdots \\ d_n \end{bmatrix}$, $\beta = \begin{bmatrix} \beta_1 \\ \beta_1 \\ \vdots \\ \beta_n \end{bmatrix}$

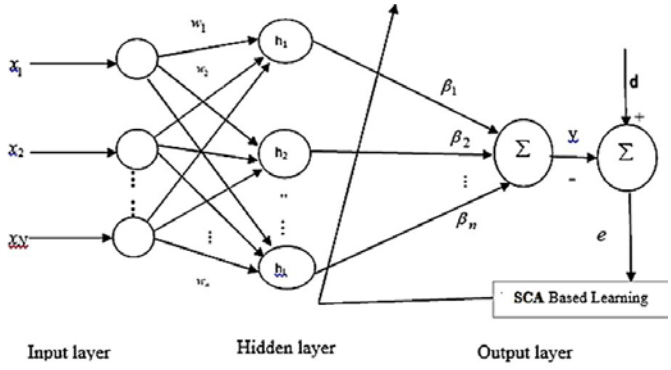


Fig. 2. SCA based WELM Model.

TABLE II. PSEUDO CODE: SCA ALGORITHM FOR WEIGHT OPTIMIZATION OF WELM MODEL

***PSEUDO CODE*:**

1. *Initialize (ELM weights) randomly.*

*2.Initialize the SCA position parameters* $\alpha_1$,$\alpha_2$, $\alpha_3$
*%Starting of the loop*

*3.Initialize the weights W of the ELM to zero*

*4.Evaluate the objective function in the next phase to evaluate fitness at first step*

*5..%Program loop*
*for i=1:n*
*for j=1:n*

$$X_{ij}^{n+1} = \begin{cases} X_{ij}^n + \alpha_1 \times sin(\alpha_2) \times |\alpha_3 y_i^n - X_i^n|, \alpha_4 < 0.5 \\ X_{ij}^n + \alpha_1 \times cos(\alpha_2) \times |\alpha_3 y_i^n - X_i^n|, \alpha_4 \geq 0.5 \end{cases}$$

*6. Update* $X_{ij}^{n+1}$ *for best fit*
*%Update the weights by using the equation*
*For j=1:n*

$$H = \begin{bmatrix} 1 & h_1(w_1; x_1) & \cdots & h_L(w_N; x_1) \\ \vdots & \vdots & \vdots & \vdots \\ 1 & h_1(w_1; x_N) & \cdots & h_L(w_N; x_N) \end{bmatrix}$$

$\beta = H^{\dagger} d$,
$H^{\dagger} = (H^T H)^{-1} H^T$

*7.end for the loop j*
*8.end for the loop i*

9. *Continue till converges, else go to step 4, and repeat until convergence is satisfied.*

## IV. Results and Discussion

### A. Database Description

The Dataset-255 is collected from "Harvard medical school of architecture (URL: http://med.harvard.edu/ AANLIB/)"[12, 39] which consists of "255 (35 normal and 220 abnormal) 256x256 axial plane brain images" are shown in Table III. "Abnormal brain MR images of Dataset-255 are from 11 types of diseases including Alzheimer's disease. The Dataset-255 consists of abnormal images of 4 new types of diseases such as chronic subdural hematoma, cerebral toxoplasmosis, herpes encephalitis, and multiple sclerosis".

TABLE III. Details of Dataset-255 [12]

| Dataset | Total number of images | | Training Images | | Testing Images | |
|---|---|---|---|---|---|---|
| | Normal | Abnormal | Normal | Abnormal | Normal | Abnormal |
| Dataset-255 | 35 | 220 | 28 | 176 | 7 | 44 |

### B. Feature Extraction

The "gray-level co-occurrence matrix (GLCM)" [40] statistical features such as "standard deviation, DM (Directional Moment), entropy, coarseness, energy, kurtosis, homogeneity, and energy" features are considered for this research work and presented in Table IV.

TABLE IV. Normalized Feature for Dataset-255

| Sl.No. | Features | Values |
|---|---|---|
| 1 | Standard Deviation | 0.4587 |
| 2 | DM | 0.8751 |
| 3 | Entropy | 0.9953 |
| 4 | Coarseness | 0.6895 |
| 5 | Energy | 0.7854 |
| 6 | Kurtosis | 0.4122 |
| 7 | Homogeneity | 0.2527 |

### C. Enhancement Results

For the enhancement of the images, the sine cosine algorithm (SCA) has been proposed and compared with the PSO and APSO techniques [34, 41].

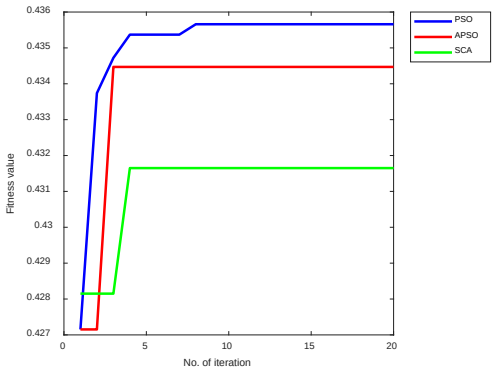


Fig. 3. Image Enhancement of the Benign Tumor Image-1 using PSO, APSO and SCA.

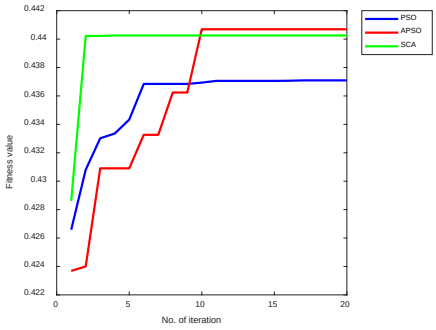


Fig. 4. Image Enhancement of the Benign Tumor Image-2 using PSO, APSO and SCA.

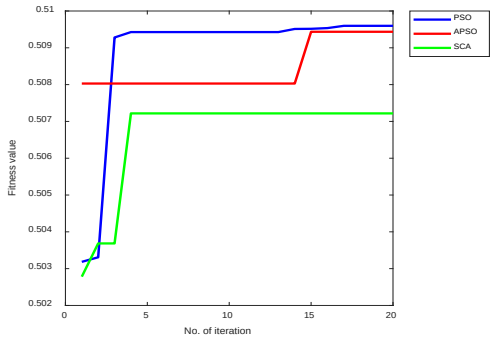


Fig. 5. Image Enhancement of the Malignant-tumor Image-1 using PSO, APSO and SCA.

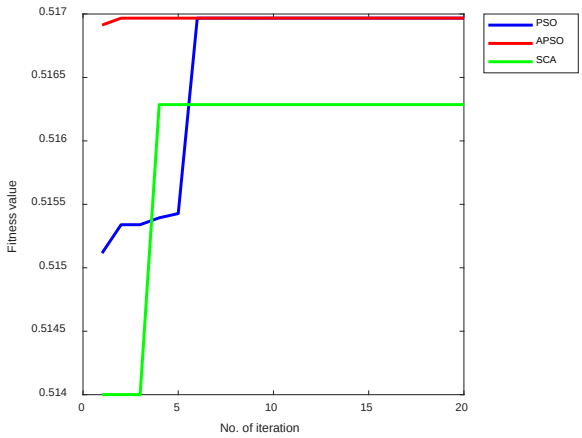


Fig. 6. Image Enhancement of the Malignant Tumor Image-2 using PSO, APSO and SCA.

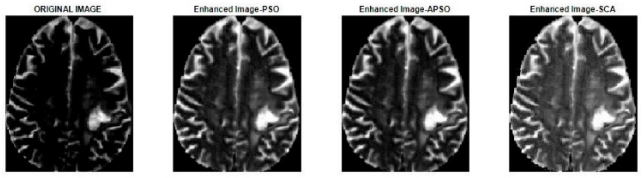


Fig. 7. Benign Tumor Image-1 Image Enhancement using PSO, APSO and SCA.

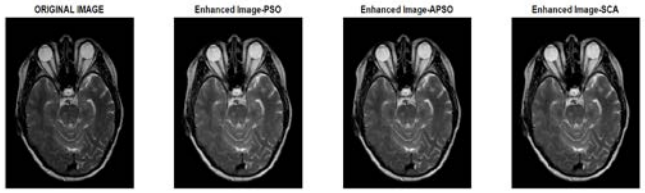


Fig. 8. Benign Tumor Image-2 Image Enhancement using PSO, APSO and SCA.

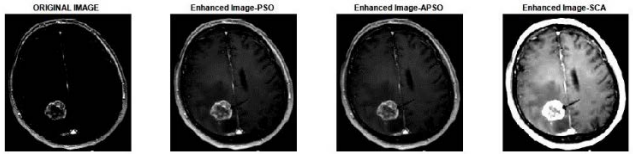


Fig. 9. Malignant Tumor Image-1 Image Enhancement using PSO, APSO and SCA.

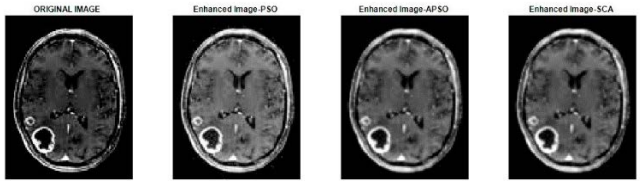


Fig. 10. Malignant Tumor Image-2 image Enhancement using PSO, APSO and SCA.

From Fig. 3 and Fig. 4, it is observed that the fitness value for SCA is 0.4318 and 0.4412 for Benign tumor image1 and image-2, which indicates better image enhancement than the other PSO and APSO methods. Moreover, from Fig. 5 and Fig. 6, it is found that the fitness value is 0.5072 and 0.5162 for malignant tumor image1 and image-2. The higher fitness values for malignant tumor images and lower values for benign tumors indicate better image enhancement of the image. Fig. 7 and Fig. 8 show the benign tumor image-1 and image -2 image enhancement using PSO, APSO, and SCA having fitness values of 0.4318 and 0.4417, and Fig. 9 and Fig. 10 show the malignant tumor image-1 and image -2 image enhancement using PSO, APSO, and SCA having fitness values 0.5072 and 0.5162. Table V presents the fitness values of Benign and Malignant tumor image enhancement.

TABLE V. FITNESS VALUES OF BENIGN AND MALIGNANT TUMOR IMAGE ENHANCEMENT

| | Fitness Value | |
|---|---|---|
| Algorithm | Benign | Malignant |
| PSO | 0.4367 | 0.5095 |
| APSO | 0.4412 | 0.5085 |
| SCA | 0.4417 | 0.5162 |

### *D. Segmentation Results*

The segmentation results are presented in Fig. 11 to Fig. 14. Fig. 11 shows the segmentation of the brain tumor using the FLICM Algorithm. It is visually observed that the noise is not reduced up to the requirement as compared to the other segmentation methods due to the fuzzy factor involvement. Fig. 12 presents the segmentation using the KWFLICM segmentation technique and the segmentation accuracy is 98.48% due to the spatial factor. Fig. 13 shows the segmentation by using the FRFCM Algorithm, which shows a better improvement in terms of accuracy to 98.84% due to the medial filtering in the fuzzy partition matrix and Fig. 14 shows the segmentation by utilizing the proposed improved FLICM technique which has higher accuracy of 99.12% due to improvement in the fuzzy factor. It is visually observed clearly that the proposed Improved FLICM technique has more noise reduction capability than the other segmentation algorithms. The segmentation accuracies are presented in Table VI.

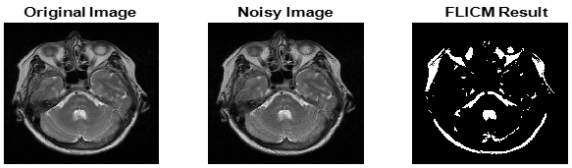


Fig. 11. Segmentation using FLICM Algorithm.

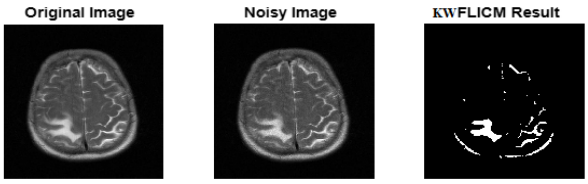


Fig. 12. Segmentation using KWFLICM Algorithm.

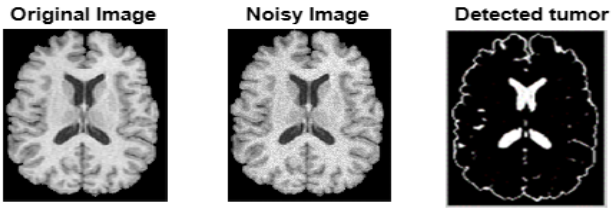


Fig. 13. Segmentation using FRFCM Algorithm.


Fig. 14. Segmentation using Proposed Improved FLICM Algorithm.

TABLE VI. IMAGE SEGMENTATION ACCURACY

| | Noise level |
|---|---|
| Algorithm | Speckle Noise |
| En FCM | 97.72 |
| FLICM | 98.11 |
| KWFLICM | 98.48 |
| NDFCM | 98.78 |
| FRFCM | **98.84** |
| Improved FLICM | **99.12** |

## E. Quality Measures

To achieve the performance comparison of segmentation, two quality measures are considered "Structural Similarity (SSIM) index and the Quality Index based on Local Variance (QILV) [12]. SSIM is sensitive to the noise and the QILV" is related to the blurring of the edges of the images. On the above, the PSNR (Peak Signal to noise ratio) is also an important parameter related to noise reduction capability. It is observed that the PSNR is 35.39 dB for the proposed FRFLICM segmentation technique which is higher in comparison to the other FCM-based segmentation techniques, which are shown in Table VII. The higher value of PSNR shows a better noise reduction capability. Moreover, the higher value of SSIM and the lower value of QILV shoe the better the segmentation performance.

TABLE VII. QUALITY MEASURES FOR THE MR IMAGE WITH SPECKLE NOISE

| | **Speckle Noise** | | |
|---|---|---|---|
| **Algorithm** | **SSIM** | **QILV** | **PSNR(dB)** |
| **En FCM** | 0.7748 | 0.7458 | 18.14 |
| **FLIFCM** | 0.7894 | 0.8248 | 22.14 |
| **KWFLICM** | 0.8287 | 0.8589 | 24.52 |
| **NDFCM** | 0.8578 | 0.8785 | 26.35 |
| **FRFCM** | **0.9101** | 0.9428 | **31.33** |
| **FRFLICM** | **0.9758** | 0.9541 | **35.69** |

## F. Classifier Performance Measure

Dataset-255 containing T2-weighted magnetic resonance brain images is considered for this research work. To avoid overfitting we have employed a 5×5 cross-validation procedure. "Sensitivity, specificity, accuracy" are the measure of system performance [12].

$$Sensitivity = \frac{TP}{TP + FN} \quad , \quad Specificity = \frac{TN}{TN + FP} \quad ,$$

$$Accuracy = \frac{TP + TN}{TP + TN + FP + FN}$$

The "5×5-fold cross-validation for each run of Dataset -255" is presented in Table VIII. Table IX shows the "5×5-fold cross validation" procedure for run-1 of Dataset-255. The calculations are considered for the modified SCA-WELM classifier.

TABLE VIII. 5×5 CROSS VALIDATION FOR EACH FOLD DATASET-255 DURING EACH RUN (SCA-WELM CLASSIFIER)

| | Fold-1 | Fold-2 | Fold-3 | Fold-4 | Fold-5 | Total | Accuracy (%) |
|---|---|---|---|---|---|---|---|
| Run-1 | 51 | 51 | 50 | 51 | 50 | 253 | **99.2156** |
| Run-2 | 51 | 51 | 50 | 50 | 51 | 253 | 99.2156 |
| Run-3 | 51 | 50 | 50 | 51 | 50 | 252 | 98.82 |
| Run-4 | 50 | 50 | 51 | 51 | 50 | 252 | 98.82 |
| Run-5 | 51 | 51 | 51 | 51 | 51 | 255 | 100 |
| Average Accuracy result | | | | | | | **99.21** |

TABLE IX. 5×5 CROSS VALIDATION OF RUN-1 FOR DATASET-255 (SCA-WELM CLASSIFIER

| Fold | Test instances | TP | FN | TN | FP | Accuracy (%) |
|---|---|---|---|---|---|---|
| Fold -1 | 51 | 43 | 1 | 7 | 0 | 98.039 |
| Fold -2 | 51 | 44 | 0 | 7 | 0 | 100 |
| Fold -3 | 51 | 43 | 1 | 7 | 0 | 98.039 |
| Fold -4 | 51 | 44 | 0 | 7 | 0 | 100 |
| Fold -5 | 51 | 43 | 1 | 7 | 0 | 98.039 |
| | Average Accuracy result | | | | | **99.21** |

TABLE X. PERFORMANCE MEASURE OF DIFFERENT CLASSIFIERS

| | Dataset -255 | | | |
|---|---|---|---|---|
| Classifier | Sensitivity | Specificity | Accuracy in (%) | Computational Time in Seconds |
| SVM | 0.96 | 0.93 | 96.85 | 256.2356 |
| ELM | 0.97 | 0.99 | 97.86 | 221.3657 |
| SCA-ELM | 0.98 | 0.93 | 98.97 | 167.1478 |
| SCA-WELM | **0.98** | **0.99** | **99.21** | **97.2576** |

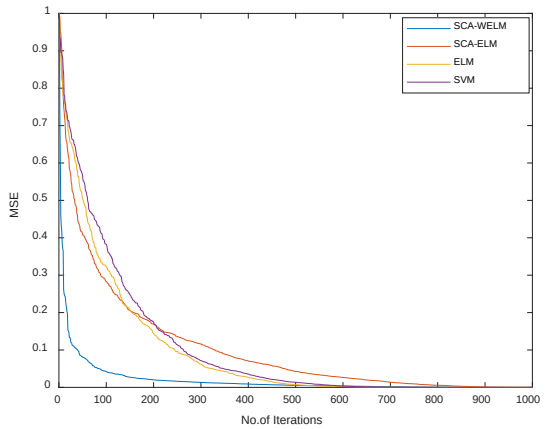


Fig. 15. Mean Square Error Results Comparison.

The proposed SCA-WELM outperforms than other mentioned classifiers in terms of "sensitivity, specificity, and accuracy". The accuracy obtained by SVM, ELM, SCA-ELM, and SCA-WELM is 0.98, 0.99, and 99.21, respectively. Computation time for the proposed SCA-WELM is achieved as 97.2576 seconds (see, Table X). For Dataset-255, it is observed from Fig. 15 that the proposed SCA-WELM model took nearly 360 iterations to converge whereas the SVM, ELM, and SCA-ELM took 530iterations, 580iterations, 430 iterations, and 330 iterations respectively. From the results of mean square error, it is confirmed that the proposed SCA-WELM model provides better performances in terms of accuracy and computational time.

## V. Conclusion

In this paper, we have proposed a sine cosine algorithm for image enhancement techniques to improve image quality. The image enhancement technique increases the contrast and smoothens the image by automatic pixel adjustment. A fast and robust FLICM-based segmentation technique has been employed to remove the speckle noise and detect the regions of the brain tumor. The comparison results are presented with other conventional EnFCM, FLICM, KWFLICM, NDFCM, and FRFCM segmentation techniques. The accuracy achieved by the proposed improved FLICM technique shows the robustness of the segmentation technique. Moreover, the higher values of SSIM and PSNR in the case of proposed improved KLICM segmentation confirm the increase in noise reduction capability. The segmented images undergo the GLCM feature extraction technique and the normalized features are presented for classification. The SCA optimization technique has been employed for the optimization of the weights of the wavelet extreme learning machine. The Mexican hat wavelet function is considered in the hidden neurons to increase the capability of classification. Dataset-255 has been considered for this research. The proposed SCA-WELM classifier model has outperformed in classifying the tumors into Benign and Malignant categories. The proposed SCA-WELM model can be applied for breast cancer, and liver tumor medical imaging classification. The proposed model will work for only features as input from the feature extraction methods, but not with images as input to the model like CNN models, which may be a drawback of the research, but this novel method can be applied for different medical images datasets. The novel level set method for 3D brain tumor segmentation [42] and active contour approaches [43] will be the future work of this research to have better visibility and comparison results.

## Acknowledgment

We acknowledge Centurion University and Technology and Management, Odisha, India, ECE department staff for availing the laboratory facility and assisted in document preparation.

## References

[1] M. Aghalari, A. Aghagolzadeh, and M. Ezoji, “Brain tumor image segmentation via asymmetric/symmetric UNet based on two-pathway-residual blocks,” Biomedical Signal Processing and Control, Vol.69, 2021, 102841. doi:10.1016/j.bspc.2021.102841.

[2] A. Sehgal, S. Goel, P. Mangipudi, A. Mehra, and D. Tyagi. “Automatic brain tumor segmentation and extraction in MR images,” Conference on Advances in Signal Processing (CASP), Vol. 24, pp.104–107, June2016, https://doi.org/10.1109/CASP.2016.7746146.

[3] N Nabizadeh, N John, and C Wright, “Histogram-based gravitational optimization algorithm on single MR modality for automatic brain lesion detection and segmentation,” EXpert Syst. Appl., Vol. 41, pp. 7820–7836.,April 2014, https://doi.org/10.1016/j.eswa.2014.06.043.

[4] Y Li, Q Dou, J Yu, F Jia, J Qin, and PA Heng, “Automatic brain tumor segmentation from MR images via a multi modal sparse coding based probabilistic model. 2015 International Workshop on Pattern Recognition in Neuro Imaging,” Vol. 26, pp.41–49. , June 2015, https://doi.org/10.1109/PRNI.2015.18.

[5] PR Pinheiro, I Tamanini, MCD Pinheiro, and VHC de Albuquerque, “Evaluation of the Alzheimer's disease clinical stages under the optics of hybrid approaches in verbal decision analysis,” Telematics Inform, Vol.35(4), pp. 776–789, Jun 2018, https://doi.org/10.1016/ j.tele.2017.04.008.

[6] A. Elazab, C. Wang, and F. Jia., “Segmentation of brain tissues from magnetic resonance images using adaptively regularized kernel-based fuzzy C-means clustering,” Computational and Mathematical Methods in Medicine, vol. 2015 (5), pp. 485–495, Jul 2015.

[7] H. Xu, C. Ye, and F. Zhang, “A medical image segmentation method with anti-noise and bias-field correction[J],” IEEE Access, Vol. 99, pp. 1, Aug 2020.

[8] A. Kouhi, H. Seyedarabi, and A. Aghagolzadeh, “Robust FCM clustering algorithm with combined spatial constraint and membership matrix local information for brain MRI segmentation,” Expert Systems with Application, Vol. 146, pp. 113159.1–113159.16, May 2020.

[9] Chao Huang, Jihua Wang, "Research on ARKFCM Algorithm Based on Membership Constraint and Bias Field Correction in Neonatal HIE Image Segmentation Method", Mathematical Problems in Engineering, Vol. 2021, pp. 587-596, Aug 2021. https://doi.org/10.1155/2021/4683609.

[10] A. Cherfa, Mokraoui, A. Mekhmoukh and K. Mokrani, "Adaptively Regularized Kernel-Based Fuzzy C-Means Clustering Algorithm Using Particle Swarm Optimization for Medical Image Segmentation," Signal Processing Algorithms, Architectures, Arrangements, and Applications (SPA), pp. 24-29, 2020, doi: 10.23919/SPA50552.2020.9241242.

[11] T Lei, X Jia, Y Zhang, L He, H Meng, and AK Nandi, “Significantly fast and robust fuzzy c-means clustering algorithm based on morphological reconstruction and membership filtering,” IEEE Trans Fuzzy Syst, Vol. 26(5), pp. 3027–3041, 2018. https://doi.org/10.1109/tfuzz.2018.2796074.

[12] Satyasis Mishra, Premananda Sahu and Manas Ranjan Senapati, “MASCA- PSO based LLRBFNN Model and Improved fast and robust FCM algorithm for Detection and Classification of Brain Tumor from MR Image” Evolutionary Intelligence, ISSN 1864-5909, Evolutionary Intelligence, Vol.12, pp.647–663 (2020) Springer https://doi.org /10.1007/ s12065-019-00266-x, July,2019,

[13] MH Kayvanrad, AJ McLeod, JS Baxter, CA Mc Kenzie and TM Peters, “Stationary wavelet transform for under-sampled MRI reconstruction. Magn. Reson. Imaging” Vol.32(10), pp:1353–64, 2016. https://doi.org/10.1016/j.mri.2014.08.004.

[14] B. Belean, R. Gutt, C. Costea and O. Balacescu, "Microarray Image Analysis: From Image Processing Methods to Gene Expression Levels Estimation," in IEEE Access, Vol. 8, pp. 159196-159205, Aug 2020, doi: 10.1109/ACCESS.2020.3019844.

[15] Wenxiu Zhao, Weiwei Wang, Xiangchu Feng, and Yu Han, “A new variational method for selective segmentation of medical images,” Signal Processing, Vol. 190, April 2022, ISSN 0165-1684. https:// doi.org/10.1016/ j.sigpro.2021.108292.

[16] ESA El-Dahshan , T. Hosny, and ABM Salem, “Hybrid intelligent techniques for MRI brain images classification,” Digit. Signal Processing, Vol. 20(2), pp. 433–41, 2010. https://doi.org/10.1016/j.dsp.2009.07.002.

[17] M Saritha, KP Joseph, and AT Mathew, “Classification of MRI brain images using combined wavelet entropy based spider web plots and probabilistic neural net-work,” Pattern Recogn. Lett.;Vol. 34(16), pp. 2151–6, Jul 2013. https://doi.org/10.1016/j.patrec.2013.08.017.

[18] G Yang, Y Zhang, J Yang, G Ji, Z Dong, and S Wang, “Automated clasification of brain images using wavelet-energy and bio geography-based optimization, Multimed. Tools Appl., Vol. 26, pp. 1–17, May 2015. https://doi.org/10.1007/s11042-015-2649-7.

[19] H Kalbkhani, MG Shayesteh, and B Zali-Vargahan, “Robust algorithm for brain magnetic resonance image(MRI) classification based on GARCH,” V ariances series. Biomed.Signal Process. Control, Vol. 8(6), pp. 909–19, Jun 2013. .https://doi.org/10.1016/j.bspc.2013.09.001.

[20] K Xiao, A Liang, HB Guan, and AE Hassanien, “Extraction and application of de-formation-based feature in medical images,” Neuro computing 2013, Vol. 120 (SupplementC), pp. 177–84. https://doi.org/10.1016/j.neucom.2012.08.054.

[21] Abd-Ellah MK, Awad AI, Khalaf AAM, and Hamed HFA, “Two-phase multi-model automatic brain tumour diagnosis system from magnetic resonance images using convolution neural networks,” EURASIPJ. Image Video Process. 2018, Vol. 97(1), pp. 1–10, May 2018. https://doi.org/10.1186/s13640-018-0332-4.

[22] H Mohsen, ESA El-Dahshan, El-Horbaty ESM, and ABM Salem. “Classification using deep learning neural networks for brain tumors,” Future Comput. Inf. J. 2018; Vol. 3, pp. 68–71, Nov 2018. https://doi.org/10.1016/j.fcij.2017.12.001.

[23] M Soltaninejad, G Yang, T Lambrou, N Allinson, TL Jones, and TR Barrick, “Automated brain tumor detection and segmentation using super piXel-based extremely randomized trees in FLAIRMRI,” Int. J. Comput. Assist. Radiol. Surg., Vol. 12(2), pp. 183–203, Feb 2017. https://doi.org/10.1007/s11548-016-1483-3.

[24] E Abdel-Maksoud, M Elmogy, and R Al-Awadi, “Brain tumor segmentation based on a hybrid clustering technique,” Egypt. Inf. J. 2015; Vol. 16(1)pp. 71–81, 2015. https://doi.org/10.1016 /j.eij.2015 .01.003.

[25] NJ Tustison, KL Shrinidhi, M Wintermark, CR Durst, BM Kandel, and JC Gee, “Optimal symmetric multimodal templates and concatenated random forests for supervised brain tumor segmentation (simplified) with ANTsR,” Neuro informatics, Vol. 13(2)pp. 209–25, April 2015. https://doi.org/ 10.1007/s12021-014-9245-2.

[26] N Nabizadeh and M Kubat, “Brain tumors detection and segmentation in MR images: Gabor Waveletvs. Statistical features,” Comput. Electr. Eng.2015; Vol. 45, (Supplement C), pp. 286–301, April 2015. https://doi.org/10.1016/j.compeleceng.2015.02.007.

[27] M Huang, W Yang, Y Wu, J Jiang, W Chen, and Q Feng, “Brain tumor segmentation based on local independent projection-based classification,” IEEE Trans. Biomed. Eng. 2014, Vol. 61(10), pp. 2633–45, 2014. https://doi.org/10.1109/TBME.2014.2325410.

[28] M Lakra and, S. Kumar, “A fractional-order PDE-based contour detection model with CeNN scheme for medical images,” J Real-Time Image Proc Vol. 19, pp. 147–160, 2022. https://doi.org/10.1007/s11554-021-01172-1.

[29] Bogdan Belean, “Active Contours Driven by Cellular Neural Networks for Image Segmentation in Biomedical Applications,” Studies in Informatics and Control, ISSN 1220-1766, Vol. 30(3), pp. 109-120, 2021. https://doi.org/10.24846/v30i3y202110.

[30] J Amin, MA Anjum, M Sharif, S Jabeen, S Kadry and P Moreno Ger, “A New Model for Brain Tumor Detection Using Ensemble Transfer Learning and Quantum Variational Classifier," Comput Intell Neurosci. 2022, Vol. 21, Vol. 42, April 2014. doi: 10.1155/2022/ 3236305. PMID: 35463245; PMCID: PMC9023211.

[31] Muhammad Arif, F. Ajesh, Shermin Shamsudheen, Oana Geman, Diana Izdrui, and Dragos Vicoveanu, "Brain Tumor Detection and Classification by MRI Using Biologically Inspired Orthogonal Wavelet Transform and Deep Learning Techniques", Journal of Healthcare Engineering, Vol. 2022, pp. 18 ,Jun 2022. https://doi.org/10.1155/2022/2693621.

[32] R.Ranjbarzadeh, , A. Bagherian Kasgari, , Jafarzadeh Ghoushchi, “Brain tumor segmentation based on deep learning and an attention mechanism using MRI multi-modalities brain images,” Sci Rep 11, 10930 Vol. 31, pp. 568-574, Aug 2021. https://doi.org/10.1038/s41598-021-90428-8.

[33] I.Abd El Kader,; Xu, G.; , Z.; Shuai, S.Saminu,; I.S.I.Javaid,;Ahmad, and S. Kamhi, “Brain Tumor Detection and Classification on MRImages by a Deep WaveletAuto-Encoder Model,” Diagnostics 2021, Vol. 11, pp. 1589, 2021. https://doi.org/ 10.3390/diagnostics11091589.

[34] SK Behera, S. Mishra and D Rana , “Image enhancement using accelerated particle swarm optimization, Int J Eng Res Techno, Vol.. l4, pp. 1049–1055, Jun 2015.

[35] M. Seyedali, “A Sine Cosine Algorithm for Solving Optimization Problems, Knowledge-Based Systems” Vol. 25, pp. 521-524, Aug 2016, doi: 10.1016/j.knosys.2015.12.022.

[36] L Szilagyi, Z Benyo, SM Szilagyii, and Adam HS, “MR brain image segmentation using an enhanced fuzzy c-means algorithm”. In: Proceeding of the 25th annual international conference of the IEEE EMBS, pp 17–21, April 2003.

[37] S Krinidis and V Chatzis “A robust fuzzy local information c-means clustering algorithm”. IEEE Trans Image Process Vol.19(5), pp. 1328–1337, Jul 2010. https://doi.org/10.1109/ tip. 2010.2040763 AQ7.

[38] E Soria-Olivas., J Gomez-Sanchis., J. D. Martin, J. Vila-Frances, M Martinez., J. R Magdalena and A. J Serrano, “BELM: Bayesian extreme learning machine,” IEEE Trans. Neural Netw., vol. 22, (3), pp. 505–509, Mar. 2011.

[39] Dataset: Webpage of Medical School of Harvard University. www.med.harvard.edu/AANLIB/home.html.

[40] DR Nayak, R Dash and B Majhi, “Discrete ripplet-II transform and modified PSO based improved evolutionary extreme learning machine for pathological brain detection,” Neurocomputing, Vol. 28, pp. 288-299, April 2016. https://doi.org/10.1016/j.neucom.2017.12.030.

[41] S.Mishra, J.Gelmecha Demissie, Ram S Singh., Davinder Singh Rathee and T Gopikrishna., Hybrid WCA–SCA and modified FRFCM technique for enhancement and segmentation of brain tumor from magnetic resonance images”, Biomedical Engineering: Applications, Basis and Communications, Vol. 33 (3), Jun 2021. DOI: 10.4015/S1016237221500174.

[42] Chaima Dachraoui, Aymen Mouelhi and Salam Labidi, “Brain MRI monitoring approach of lesion progress in multiple sclerosis using active contours,” International Journal Of Modelling Identification And Control Vol. 38 (1), pp. 32-45, 2019.

[43] A Khosravanian, M.Rahmanimanesh, and P. Keshavarzi, “Level set method for automated 3D brain tumor segmentation using symmetry analysis and kernel induced fuzzy clustering,” Multimedia Tools Appl 81, pp. 21719–21740, April. 2022. https://doi.org/10.1007/s11042-022-12445-7.